



# Thermal performance and energy cost of Korean multispan greenhouse energy-saving screens

Anis Rabiu<sup>a</sup>, Misbaudeen Aderemi Adesanya<sup>a</sup>, Wook-Ho Na<sup>b</sup>, Qazeem O. Ogunlowo<sup>a</sup>, Timothy D. Akpenpuun<sup>b,c</sup>, Hyeon Tae Kim<sup>d</sup>, Hyun-Woo Lee<sup>a,b,\*</sup>

<sup>a</sup> Department of Agricultural Civil Engineering, College of Agricultural and Life Sciences, Kyungpook National University, Daegu, 702-701, South Korea

<sup>b</sup> Smart Agriculture Innovation Centre, Kyungpook National University, Daegu, 41566, South Korea

<sup>c</sup> Department of Agricultural and Biosystems Engineering, University of Ilorin, PMB 1515, Ilorin, Nigeria

<sup>d</sup> Department of Bio-Industrial Machinery Engineering, Gyeongsang National University, Jinju, 52828, South Korea

## ARTICLE INFO

Handling Editor: X Zhao

**Keywords:**

Climate screens properties  
Greenhouse farming  
Thermal performance  
Energy saving  
Energy cost  
TRNSYS

## ABSTRACT

Protected agricultural system such as a greenhouse cultivation is increasingly replacing traditional farming systems. Nonetheless, high energy demand in greenhouse farming requires innovative technologies through the use of climate screens to ensure sustainable production. Thus, this study developed a novel methodology for examining the energy retention capacity and economic effectiveness of greenhouse climate screen materials using their thermophysical, radiometric and aerodynamic properties in TRNSYS software. The TRNSYS model was developed to determine the energy consumption, which was validated using a multi-span Venlo-type experimental greenhouse (Yeoju, South Korea). Further analyses on energy saving capacity of different screens and the equivalent energy costs were performed. The results from this research showed that among the fifteen investigated screens, the ensemble screen (M3) saved 34.09 kWh.m<sup>-2</sup> of annual energy, equivalent to 60 % of the heating energy demand, and energy cost of 4490.26 Korean won. m<sup>-2</sup>. Further, the results revealed that the climate screens with multi-layer, thermoreflective, low longwave transmissivity, impermeable and aluminized strips or surface characteristics and features have a considerable impact on reducing greenhouse energy use and desirable for high energy-saving. This research has demonstrated that the techniques and methods utilised can investigate all the types of covering and thermal screens used in greenhouse.

## 1. Introduction

Greenhouse cultivation offers immense potential for global food security as it boosts crop growth by limiting (controlling) the influence of the atmospheric environment on cultivating envelope [1]. It is an anti-seasonal controlled structure that provides a conducive atmosphere to grow vegetables and fruits, protect crops against the effects of severe weather conditions, pests, and diseases, and improve the quality of crop production [2]. However, this controlled cultivation system is directly affected by the high energy demand for heating and cooling during winter and summer, respectively [3]. The greenhouse energy consumption is high and constitutes a large percentage of the cultivation inputs. The annual energy consumption has been estimated to be 50 % of the total production cost [4–6]. Thus, high energy load is one of the

prime challenges that hinder the enormous prospects of this agricultural system, mostly in regions of adverse climatic conditions [7]. In fact, greenhouse farming is referred to as one of the most energy-intensive sectors in the agricultural industry [8]. High energy demand in greenhouse increases fossil fuel consumption, grid electricity input, and operating costs while contributing to global gas emissions and global warming [9]. The global energy demand has continuously increased, it has been estimated to rise by 37 % in 2040 [10], and greenhouse energy demand will constitute a significant proportion of the total demand. Therefore, renewable energy methods that will improve greenhouse energy conversation and enhance sustainable energy strategies in the agricultural sector are urgently required [11].

Several renewable energy technologies are utilised to reduce the huge energy demand, such as photovoltaic (PV) modules, solar thermal collectors, hybrid PV/T collectors and systems, phase change material

\* Corresponding author. Department of Agricultural Civil Engineering, College of Agricultural and Life Sciences, Kyungpook National University, Daegu, 702, South Korea.

E-mail addresses: [rabiuanis@knu.ac.kr](mailto:rabiuanis@knu.ac.kr), [rabiuanis@gmail.com](mailto:rabiuanis@gmail.com) (A. Rabiu), [misbauadesanya@knu.ac.kr](mailto:misbauadesanya@knu.ac.kr) (M.A. Adesanya), [wooks121@knu.ac.kr](mailto:wooks121@knu.ac.kr) (W.-H. Na), [ogunlowoqazeem@knu.ac.kr](mailto:ogunlowoqazeem@knu.ac.kr) (Q.O. Ogunlowo), [akpenpuun.td@unilorin.edu.ng](mailto:akpenpuun.td@unilorin.edu.ng) (T.D. Akpenpuun), [bioani@gnu.ac.kr](mailto:bioani@gnu.ac.kr) (H.T. Kim), [whee@knu.ac.kr](mailto:whee@knu.ac.kr) (H.-W. Lee).

<b>Nomenclature</b>	
<b>Symbols</b>	
ACH	Air change per hour, ( $\text{h}^{-1}$ )
$C_{\text{cover}}$	Cloudiness factor of the sky
Ce	Fuel unit cost
$C_{\text{fuel}}$	Annual fuel demand
$CF_1$	Cashflow from energy-savings
Cp	Specific heat capacity of air, ( $\text{kJ K}^{-1} \text{kg}^{-1}$ )
$E_b$	The emissive power of the black fabric, ( $\text{W m}^{-2}$ )
$E_s$	The emissive power of the thermal screen, ( $\text{W m}^{-2}$ )
$f_{s,\text{sky}}$	Fraction of the sky seen by the outside surface
$h_{\text{conv}}$	Convective heat transfer coefficient ( $\text{kJ h}^{-1} \cdot \text{m}^{-2} \text{k}^{-1}$ )
IC	Initial invested capital
i	Interest rate
DPP	Discounted Payback Period
$Q_{\text{conv}}$	Convective heat transfer, (W)
$Q_{\text{rad}}$	Radiative heat loss to the surface, (W)
$Q_{\text{inf}}$	Heat loss through the screen pore, (W)
$Q_a$	Inward sky radiation toward the thermal screen, ( $\text{W.m}^{-2}$ )
$Q_b$	Upward radiation from the thermal screens to the sky, ( $\text{W.m}^{-2}$ )
$Q_c$	Upward longwave radiation from the thermal screen toward the black fabric, ( $\text{W.m}^{-2}$ )
$Q_d$	Inward longwave radiation toward the thermal screen from the black fabric, ( $\text{W.m}^{-2}$ )
r	Dynamic discount rate
$S_a$	Sky downward shortwave radiation, ( $\text{W.m}^{-2}$ )
$S_b$	Outward shortwave radiation toward the sky from the thermal screen, ( $\text{W.m}^{-2}$ )
$S_c$	Outward shortwave radiation from the thermal screen toward the black fabric, ( $\text{W.m}^{-2}$ )
$S_d$	Shortwave radiation from the black fabric toward the thermal screen, ( $\text{W.m}^{-2}$ )
$T_a$	Ambient temperature, ( $^{\circ}\text{C}$ )
$T_i$	Inside air temperature, ( $^{\circ}\text{C}$ )
$T_{\text{is}}$	Inside surface temperature, ( $^{\circ}\text{C}$ )
$T_{\text{os}}$	Outside surface temperature, ( $^{\circ}\text{C}$ )
$T_{\text{fsky}}$	Fictive sky temperature used for longwave radiation, ( $^{\circ}\text{C}$ )
$T_{\text{grd}}$	Fictive ground temperature used for longwave radiation, ( $^{\circ}\text{C}$ )
$T_{\text{sky}}$	Effective sky temperature, ( $^{\circ}\text{C}$ )
V	Airflow rate, ( $\text{m}^3 \cdot \text{s}^{-1}$ )
<b>Greek symbols</b>	
$\alpha_L$	Longwave absorptivity of the thermal screen
$\varepsilon_b$	Emittance of black fabric
$\varepsilon_0$	Emittance of the clear sky
$\mu$	Denotes $10^{-6}$
$\rho$	Air density, ( $\text{kg.m}^{-3}$ )
$\rho_b$	Reflectance of black fabric
$\rho_L$	Longwave reflectance of the thermal screen
$\rho_s$	Reflectance of the thermal screen
$\sigma$	Stephen-Boltzmann constant ( $\text{W.m}^{-2} \cdot \text{k}^{-4}$ )
$\tau_b$	Transmittance of black fabric
$\tau_L$	Longwave transmittance of the thermal screen
$\tau_s$	Transmittance of the thermal screen
<b>Abbreviations</b>	
ASHRAE	American Society of Heating, Refrigerating and Air-conditioning
AED	Annual Energy Demand (kWh)
BES	Building energy simulation
EEV	Equivalent Energy Value ( $\text{L.kWh}^{-1}$ or $\text{m}^3 \cdot \text{kWh}^{-1}$ )
KMA	Korean Metrological Administration
KPI	Korean Price Information
KRW (Won)	Korean won
LBLN	Lawrence Berkeley National Laboratory
LPG	Liquefied Petroleum Gas
QTM-500	Quick thermal meter
TRNSYS	Transient system simulation

(PCM) and underground based heat storage techniques, energy-efficient heat pumps, alternative facade materials for better thermal insulation (thermal screens, climate screens) and power generation (heat insulation solar glass, PV glazing, aerogel and vacuum insulation panel, polycarbonate sandwich panels), innovative ventilation technologies using pre-heating and cooling (high performance windcatchers) and efficient lighting systems, are used to create an energy-efficient greenhouse system and to achieve a net-zero greenhouse production [2,12]. These renewable energy technologies are grouped into passive and active energy [13], and climate screen (i.e., thermal screen, shading screen, thermal blanket and thermal curtain) materials are one of the most efficient types of passives, renewable, and sustainable energy techniques for greenhouse energy saving [4]. These passive heating methods prevent and maintains heat loss to the ambient environment at nighttime, mostly during winter, whereas passive cooling regulates excess solar radiation concentration in the greenhouse microclimate during daytime from the greenhouse [4]. Studies from literature have reported a general estimated ratio of the energy-saving percentage of these screens materials [7] reported an estimated value that thermal screens can reduce 40%–70% of nighttime longwave radiation and save 23%–60% of heating energy by reducing the heated air in the greenhouse microenvironment. Moreover, 90% of energy saving can be achieved depending on the type of thermal screens, geographical location, and passive heating system [14]. The thermal and shading systems in the greenhouse account for a significant percentage of overall energy consumption [15–17]. None of these studies discussed specifically the

energy-saving capacity of individual screen materials.

Greenhouse covering materials are transparent that envelope the greenhouse side walls and roof for admitting and allowing the transmission of solar radiation into the greenhouse for photosynthesis and maintaining the internal temperature [18]. These materials have lower thermal retention capacity and do not prevent night radiative heat loss to the ambient environment. Thus, this resulting to the utilization of the thermal screens in greenhouses as a technological and renewable solution to reduce energy loads (heating and cooling) by preventing excessive radiative heat loss during the nighttime and limiting the excessive transmission of solar radiation during the day time [19]. [13] investigated the heat transfer phenomenon of the greenhouse, which describes distinct heat loss patterns and mechanisms. The moveable thermal screen serves as a buffer to reduce the volume of space to be heated in the greenhouse during winter by reducing convective heat loss and minimizing radiative heat loss during nighttime [16,20]. It also creates stable microclimate conditions by reducing the influences of solar radiation and night sky radiation [21–23]. The shading screens are mostly employed in summer during the day to reduce the quantity of solar radiation coming into the greenhouse to manage heat buildup [21]. Thermal screen is a nighttime insulation curtain deployed either internally or externally in a greenhouse during winter to reduce or prevent heat loss due to radiation and convection to the ambient atmosphere [24]. Thermal screens are usually retract (close) during the day to allow the transmission of solar radiation inside the greenhouse for photosynthesis and thermal gains. Moreover, shading screens are mostly

applicable in summer to control and reflect excess solar radiation entering the greenhouse [12].

Transient simulation system (TRNSYS) is a building energy simulations (BES) that is a versatile energy simulation tool for simple and complex systems. It is capacity of investigating the energy analysis of single and multi-zone buildings [25]. This software is developed and frequently used for simulation, optimization and thermal system of commercial, residential and industrial buildings. However, due to unavailability of some specific greenhouse features (thermal screen) in the software library, the application of TRNSYS in greenhouse has not been extensively explored [25,26]. Energy management is one of the main challenges in greenhouse production and several studies have utilised various energy models to investigate the heating and cooling load of greenhouse. [26] studied the effect of greenhouse design parameters on energy load, thermal requirements, and energy consumption using TRNSYS. The TRNSYS software was also used to examine the impact on the thermal behaviour and infiltration of buildings by [27]. Hence [28], developed TRNSYS model to evaluate the effect of design orientation on the thermal behaviour and energy load of the Agadir Moroccan greenhouse situations. Due to lack of some greenhouse features in the energy simulation models, greenhouse simulation were conducted with constant parameters and assumptions, this resulting to high predicting errors. [25] reported that simulation of greenhouse heating load with specified features (thermal screen and plants) excluded could result in a larger prediction errors and inaccuracy from 33% to 68%.

The dynamic nature of the greenhouse envelope, plant, and thermal screen materials complicates the modelling of greenhouse thermal microclimates using building energy software. Thus, few researchers have investigated the properties of greenhouse-covering materials in order to improve the energy prediction efficiency of the transient models. [29] quantify the percentage the longwave radiation by measuring radiative properties of greenhouse thermal screens at the nighttime. The radiation balance approach was used to investigate the convective heat transfer coefficients of greenhouse thermal screens under a natural conditions [30]. [31] used wide-range spectral radiation to calculate the radiative properties of greenhouse plastic covering and energy management. The hotbox method was used to determine the overall heat transfer coefficient of greenhouse covering, and its thermal properties [32,33]. Furthermore, the study determined the effect of condensation on energy-saving. In addition, the radiometric and thermal properties of greenhouse covering materials were studied to determine the effects of transmissivity, reflectivity, and absorptivity on energy-saving [34]. However, none of these studies considered the application of this properties to investigate the thermal efficiency of screens in a greenhouse model. [26] used a single-span TRNSYS greenhouse model to optimized the energy conversation of Luxous and Tempa screen materials. These studies only considered the radiometric and thermal properties but ignored the effects of aerodynamic properties on the materials selected for the research. Using the TRNSYS hotbox model, [35] investigated the overall heat transfer coefficient to describe the thermal retention capacity of greenhouse energy screens. Thus, the study used screen properties which includes thermophysical, radiometric, and aerodynamic in the Hotbox model. Nevertheless, the research did not consider the application of screen properties for a real-time condition in the greenhouse TRNSYS model. Furthermore, [36] utilise the KASPRO energy model to investigated greenhouse screen properties and determine the energy savings under a defined condition using screen aerodynamic and thermal properties alone. The consideration and presence of climate screens in most energy simulation model are usually ignored due to unavailability of this screen material properties in TRNSYS software.

To the best of our knowledge, there is no existing study that investigated the precise methods to quantify the properties, energy retention capacities, and thermal performance of greenhouse energy-saving screens in a real-time scenario using the greenhouse TRNSYS model, especially in South Korea. As a consequence, the objective of this

research endeavor was to develop a novel methodology approach, pertinent tools, tailored for evaluating the properties (including thermophysical, radiometric and aerodynamic properties) of climate screen materials. Simultaneously, the study determines the potentials for energy-saving in terms of energy performance (retention capacity) through the utilization of building energy simulation software. These methods can be universally utilised to examine any greenhouse covering and thermal screen of different types. The research involves a comparative validation between the Yeoju experimental greenhouse and the energy demand and savings derived from the TRNSYS model. To determine energy costs, the research employs energy-saving percentages coupled with the energy tariffs specific to major energy carriers (namely electricity, diesel, gasoline, and liquefied petroleum gas LPG) within the Korean context. The rationale for choosing the TRNSYS software stems from its adaptability and expansive applicability in modelling and simulating greenhouse energy loads, thereby enabling comprehensive analyses of microclimate energy management. By adopting this systematic approach, the integration of climate screens into the TRNSYS model permits precise and accurate predictions of greenhouse systems. This initiative opens doors to scrutinising screen performance, which remains hitherto unexplored in existing literature.

The outcomes of this research hold considerable potential to benefit greenhouse farmers, growers, manufacturers, researchers, and practitioners. The insights gleaned from this study can facilitate informed investment decisions and design choices. Furthermore, it paves the way for advancements in energy screen selection, thereby fostering efficient, resource-conserving, and sustainable practices within greenhouse crop cultivation.

## 2. Materials and methods

### 2.1. Greenhouse screen material properties

#### 2.1.1. Material selection and thermophysical properties

**Fig. 1** indicates 15 commercial greenhouse energy screen materials commonly used in the South Korean market and mostly utilised by greenhouse farmers, which were selected for this study to investigate the material properties and prediction of energy-saving capacity in the thermal modes of a greenhouse model. The screen materials were classified into the thermal screen, shading screen, and thermal insulator. Some of these materials were combined to form a single-layer multi-material energy screens (M1, M2, and M3). The compositions and arrangements of these materials were discussed in the previous research [35]. Moreover, this subchapter measures the thermophysical properties of greenhouse energy screen materials, which include, screen thickness, thermal conductivity, and physical feature characteristics. An electronic digital calliper and a quick thermal meter (QTM-500) were used to determine the screen thickness and thermal conductivity, respectively [37,38]. Furthermore, the output properties of the screens were input into the TRNSYS model through the TRNBuild software via the DOE-2 file generated by Windows 7.8 software of the Lawrence Berkeley National Laboratory (LBNL).

#### 2.1.2. Radiometric properties

The radiometric properties of the greenhouse energy screen were determined using the radiation balance method [29,35,39]. Radiation balance experiments were conducted during nighttime and daytime to determine longwave and shortwave radiation fluxes on the screen materials, respectively. This experiment was conducted in two winter seasons between January 2020 and March 2021 and between December 2021 and March 2022 with the aid of different radiation sensors, including a net radiometer, a pyranometer, and pyrgeometer sensors. These sensors were installed on a radiometric balance steel stand, which was fabricated by aluminium steel, as shown in **Fig. 2**. The stand had dimensions of 2 m by 2 m by 1.5 m (length width height). The sensors were installed at a height of 0.75 m from the stand base, which is

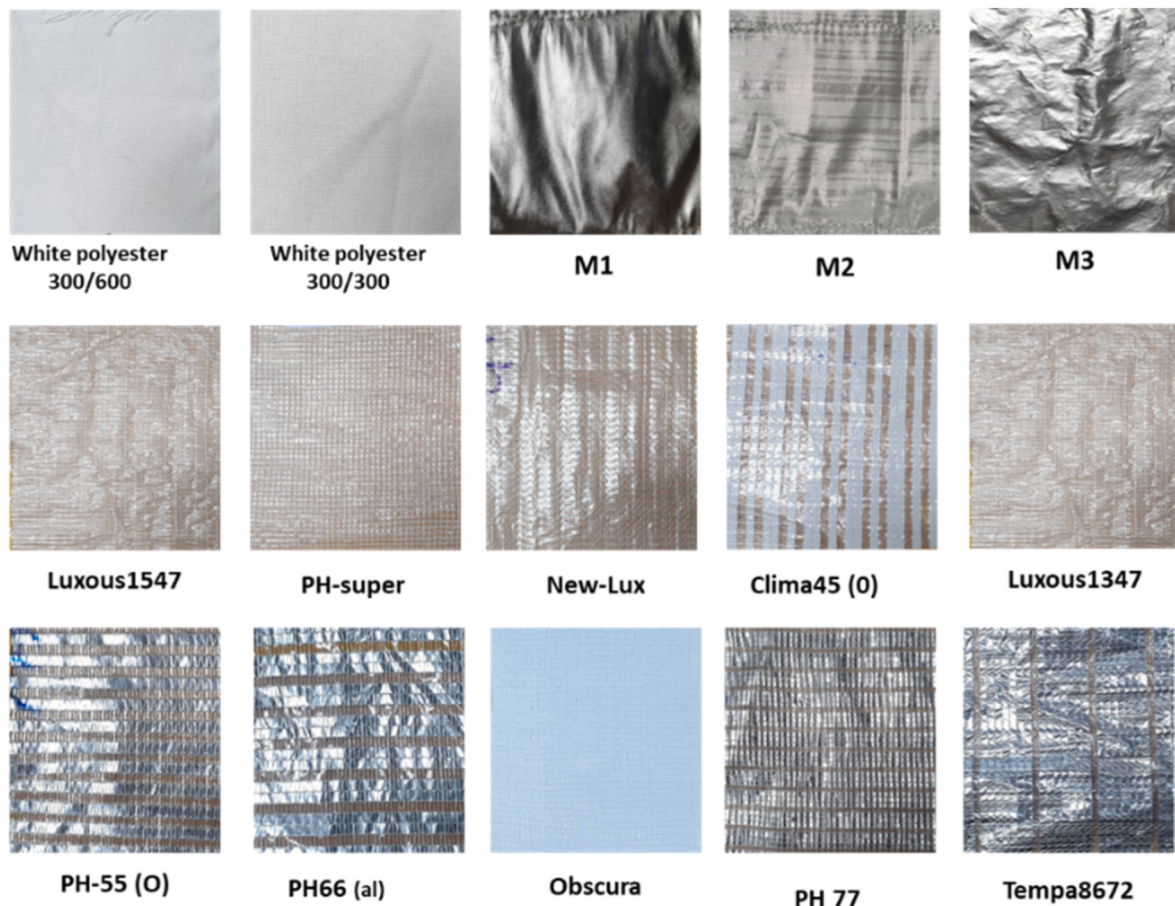


**Fig. 1.** Overview of greenhouse energy-efficient screen materials used in the study.

between the thermal screen under investigation and black fabric and 1.25 m above the thermal screen and below the sky.

The shortwave radiation was measured during the daytime between 0600 h and 1800 h, whereas the longwave radiation was recorded between 1800 h and 0600 h of the subsequent day. Fig. 2A represents the radiation balance during the nighttime, and Fig. 2C shows the experimental real-time situation. Eqs. (1)–(4) represent the radiation balance equation shown in Fig. 2A, [12,21,29,34,35,39–41].

$$Q_b = E_s + (\rho_L \times Q_a) + (Q_d \times \tau_L) \quad (1)$$

$$Q_c = E_s + (\tau_L \times Q_a) + (Q_d \times \rho_L) \quad (2)$$

$$Q_d = E_b + [(\rho_b + \mu) \times E_s] + [(\rho_b - \mu) \times (\rho_L \times Q_d)] + [(\rho_b - \mu) \times (\tau_L \times Q_a)] \quad (3)$$

$$\alpha_L = 1 - (\rho_L + \tau_L) \quad (4)$$

Conversely, Fig. 2B depicts the shortwave radiation scenario, and Fig. 2D represents the experimental stand during the daytime. The shortwave radiation balance equation is described by Eqs. (5) and (6) [35,41]:

$$S_b = (\rho_s \times S_d) + (\tau_s \times S_d) \quad (5)$$

$$S_c = (\rho_s \times S_d) + (\tau_s \times S_a) \quad (6)$$

The MATLAB software (MATLAB 22B, MathWorks, USA) was used for the computation and solving the complex equations simultaneously when the number of unknowns equalled the number of the equations. The longwave and shortwave reflectance, emittance, and transmittance were obtained from Eqs. (1)–(4), and Eqs. (5) and (6), respectively.

Furthermore, the output radiometric properties of the screen obtained from this experiment were input into the TRNSYS model through the TRNBuild software via the DOE-2 file generated by Windows 7.8 software of the LBNL.

To record the longwave and shortwave radiation, the following sensors were employed; Two Kipp and Zonen NR Lite2 Net radiometer (Netherlands) sensitivity  $10 \mu\text{V W}^{-1} \text{m}^{-2}$ , response time  $<20$  s, sensor asymmetry  $<15\%$ , units  $\text{W.m}^{-2}$ , Kioki data logger LR-5042 (Japan), and spectral range 0.2–100  $\mu\text{m}$ . Four Kipp and Zonen CPM3 pyranometer (Netherlands) sensitivity  $11.54 \mu\text{V W}^{-1} \text{m}^{-2}$ , response time  $<18$  s, temperature sensitivity  $-10$  to  $+40$ , tilt error  $<2\%$ , zero offset  $<15 \text{ W.m}^{-2}$ , Kioki data logger LR-5042 (Japan), Spectral range between 300 and 2800 nm. Two Kipp and Zonen CGR3 pyrgeometer (Netherlands) sensitivity  $14.54 \mu\text{V W}^{-1} \text{m}^{-2}$ , response time  $<18$  s, tilt error  $<2\%$ , zero offset  $<5 \text{ W m}^{-2}$ , Campbell scientific Model CR300 data logger (Inc. USA) spectral range of 4.5–42  $\mu\text{m}$ .

### 2.1.3. Aerodynamic property

Greenhouse energy screen materials are either permeable or impermeable, and the permeability of the material dictates the airflow rate through screen pores. This directly impacts the air exchange and the quantity of heat and energy losses or retained due to infiltration heat loss [36]. An air-suction device consisting of a draining water tank system was developed to determine the permeability of the energy screen, as displayed in Fig. 3A. The tank is operated on the mechanism of air–water flow suction, which was aided by gravitational forces. The air-suction device works by draining the water tank, which induces air into the closed system when valve C is opened, and the air runs through valve A (inlet air pipe), which accommodates the screen material at the gate entrance, as shown in Fig. 3B. The screen material installed causes a

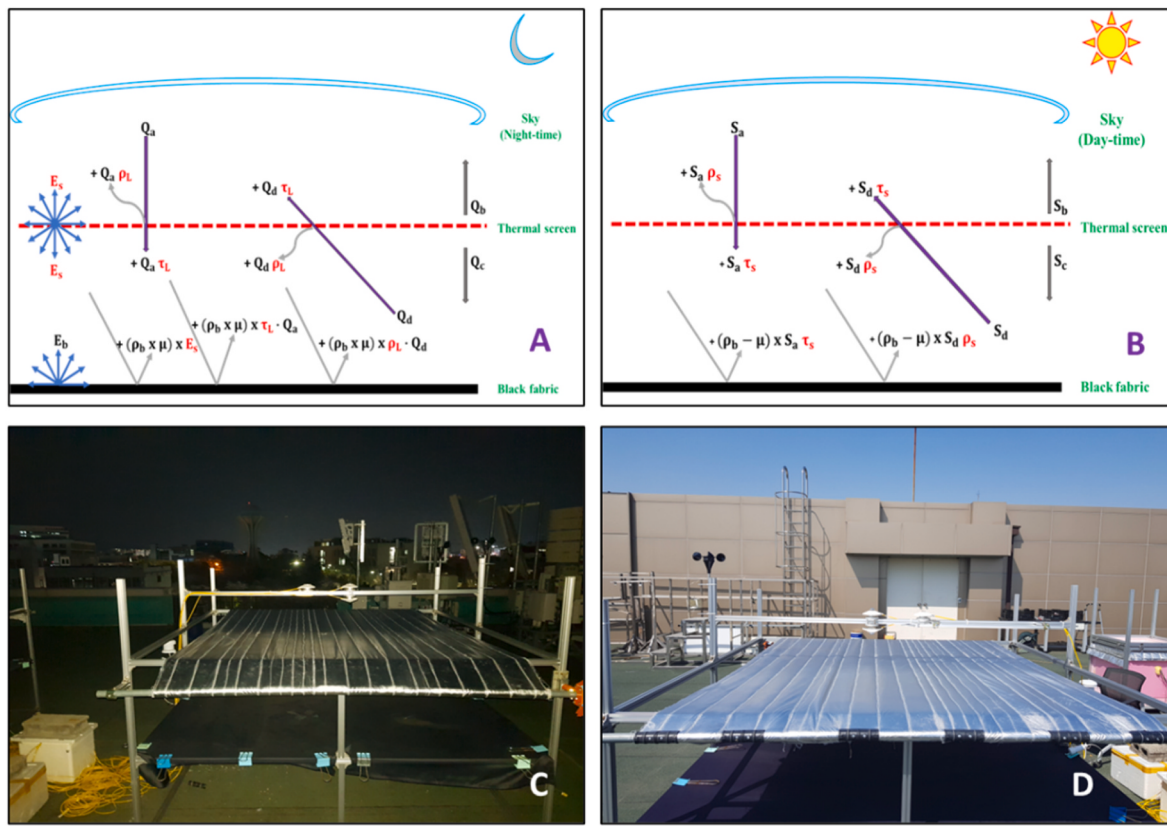


**Fig. 2.** (A) Schematic diagram of incoming and outgoing longwave radiation, (B) shortwave radiation, and (C) experimental setup for determining the radiometric properties of screens during the daytime and (D) nighttime [12,35].

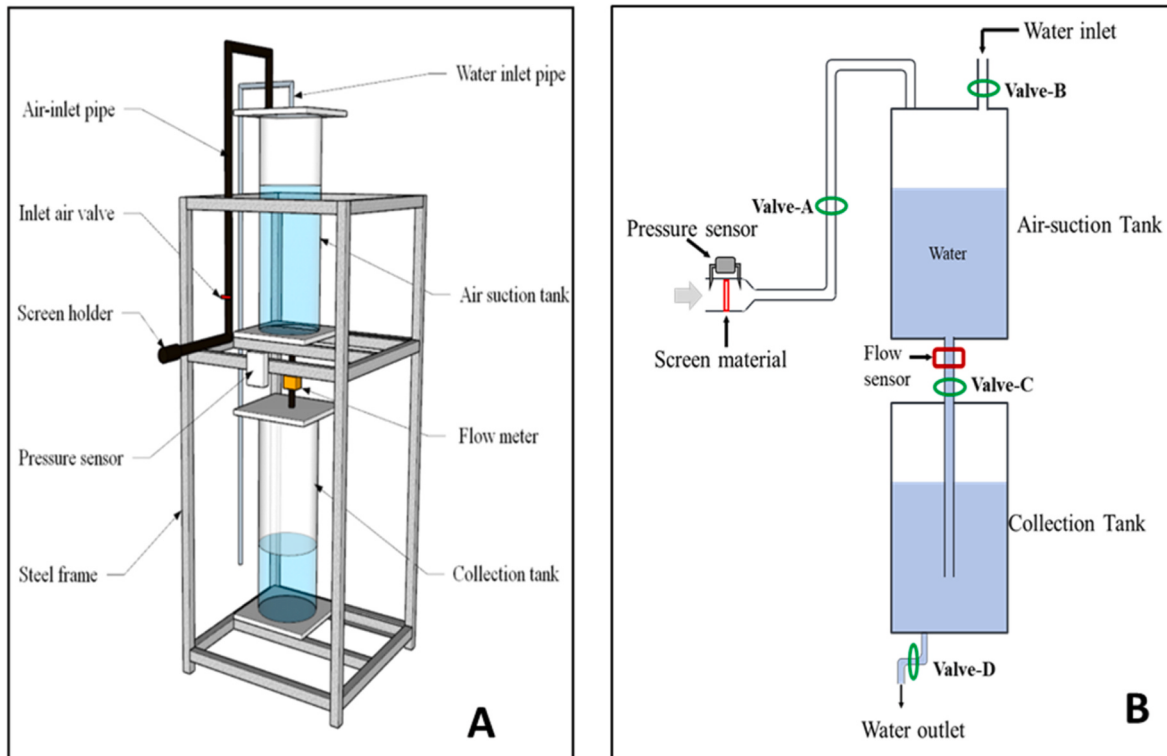


**Fig. 3.** (A) CAD design of the air-suction device and (B) schematic diagram of the air-suction device.

pressure drop due to air suction between the outer and inner surfaces of the screen [35,42–46]. The porosity of each material determines the amount of air velocity moving during an experimental cycle [47,48]. Thus, the differential pressure sensor metered the pressure difference, while the water flowing out of the system was measured at valve C to quantify the volume of the air sucked into the system. The detailed step-by-step procedure used for calculating the aerodynamic properties of a greenhouse screen by the air-suction method follows [35].

The infiltration flow rate obtained from this investigation was converted to air change per hour (ACH). The ACH values computed from this experiment were input into the TRNBuild software, which defines the infiltration rate of each screen material when applied to the model.

## 2.2. Description of the experimental greenhouse

The experimental greenhouse site is located at Ohak-dong, Yeoju-si, Gyeonggi-do, western province, South Korea. The farm has a floor area of 3942 m<sup>2</sup>, which is separated by horticulture glass (HG) and thermal curtain (Obscura) into farm A and farm B, which are 2160 m<sup>2</sup> and 1782 m<sup>2</sup>, respectively. The greenhouse is a multi-span Venlo type, as shown in Fig. 4, with dimensions of 32 m × 67.5 m × 7.25 m and 36 m × 49.5 m × 7.25 m for farms A and B, respectively. Additionally, the greenhouse roof and side walls were covered with Fluorine film and horticulture glass (HG, 4 mm), respectively. Thus, the inner thermal screens were installed both horizontally and vertically. The horizontal energy screens were Luxous1547 and Tempa (commercial names), which were positioned on the first and second layers under the roof, whereas the vertical energy screens were Obscura, which are installed in front of the inner walls. The greenhouse inner microclimate is horizontally segregated into 3 different zones due to the deployment (open) of the energy screens, and when all the screens are retracted (closed), it maintains a single zone (which is the full volume capacity of the greenhouse). During winter, the greenhouse regularly maintains a three-zone condition for passive insulation, and the two layers of the energy screen are deployed simultaneously, whereas, during summer, the greenhouse maintains a single-or-two-zone situation for reducing excess solar radiation intensity. The deployment and retraction of the screen are more frequent in this season for shading when the solar radiation intensity is above 0.5 kW m<sup>-2</sup>. Furthermore, onsite greenhouse microclimate weather parameters were measured and recorded, which include inside and ambient temperature, relative humidity, and solar radiation, using sensors and data loggers. The ambient weather data were also obtained from the Korean Meteorological Association for the simulation.

## 2.3. Greenhouse model and energy demand

TRNSYS is one of the versatile dynamic BES tools and a component-



**Fig. 4.** Aerial view of the Yeoju experimental greenhouse.

based building and energy simulation software. This software was employed for modelling and simulating the experimental greenhouse microclimate, as presented in Fig. 5. The Yeoju greenhouse model was applied to investigate the energy load and energy efficiency of the greenhouse and further examine the energy-saving capacity of the screen materials. The properties of screen materials were measured as explained above (section 2.1), which includes the thermophysical, radiometric, and aerodynamic properties. The results of the screen properties from these experiments were processed into a DOE-2 data file format using the LBNL Windows 7.8 software and then imported into the TRNBuild software. Furthermore, the geometry of the greenhouse, as shown in Fig. 5, was developed using Transys3D, an add-in used in SketchUp design software, and compiled as a file in the ".idf" format. This file was then imported into TRNBuild (the building editable interface of the TRNSYS software), and it defines the properties of all other components in the greenhouse. The TRNBuild ".b18" file is further imported into the TRNSYS software through the building component (Type 56) [49]. The TRNSYS model works on the combination and linkage of BES components, as indicated in Fig. 6, which displays the interface of the TRNSYS simulation studio. The interface comprises the building, weather, greenhouse control, ventilation, and scheduling components.

All the heat transfer calculations were performed in this component. Eqs. (7) and (10) describe convective and radiative heat transfer, respectively, for the greenhouse, and the infiltration heat loss is represented by Eq (11), [49–51].

$$Q_{\text{conv}} = h_{\text{conv}} (T_{os} - T_{is}) \quad (7)$$

$$Q_{\text{rad}} = \sigma \varepsilon_0 (T_{os}^4 - T_{sky}^4) \quad (8)$$

$$T_{sky} = (1 - f_{s,sky}) \times T_{grd} - f_{s,sky} \times T_{sky} \quad (9)$$

$$T_{sky} = T_a [\varepsilon_0 + 0.8 (1 - \varepsilon_0) C_{cover}]^{0.25} \quad (10)$$

$$Q_{\text{inf}} = V \rho C_p (T_i - T_a) \quad (11)$$

### 2.3.1. Simulation of the greenhouse microclimate zones

The greenhouse model runs a series of simulations to determine the energy demand in terms of cooling and heating load from the period between 1 January 2022 to 31 December 2022 while maintaining the inside temperature of the greenhouse at 15 °C throughout the year. In winter, the greenhouse maintained a three-zone scenario owing to the deployment of the energy screens, whereas during summer, the screen(s) were retracted to a single zone or two zones depending on the inside temperature and solar radiation intensity. The greenhouse single-zone scenario occurs without thermal screens, and this condition has no buffer zone for nighttime heat loss. The two horizontal screens are

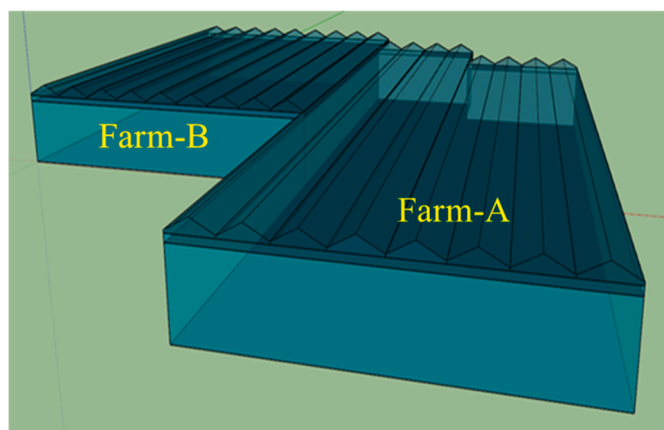


**Fig. 5.** Trnsys3d sketch diagram of the Yeoju experimental greenhouse.

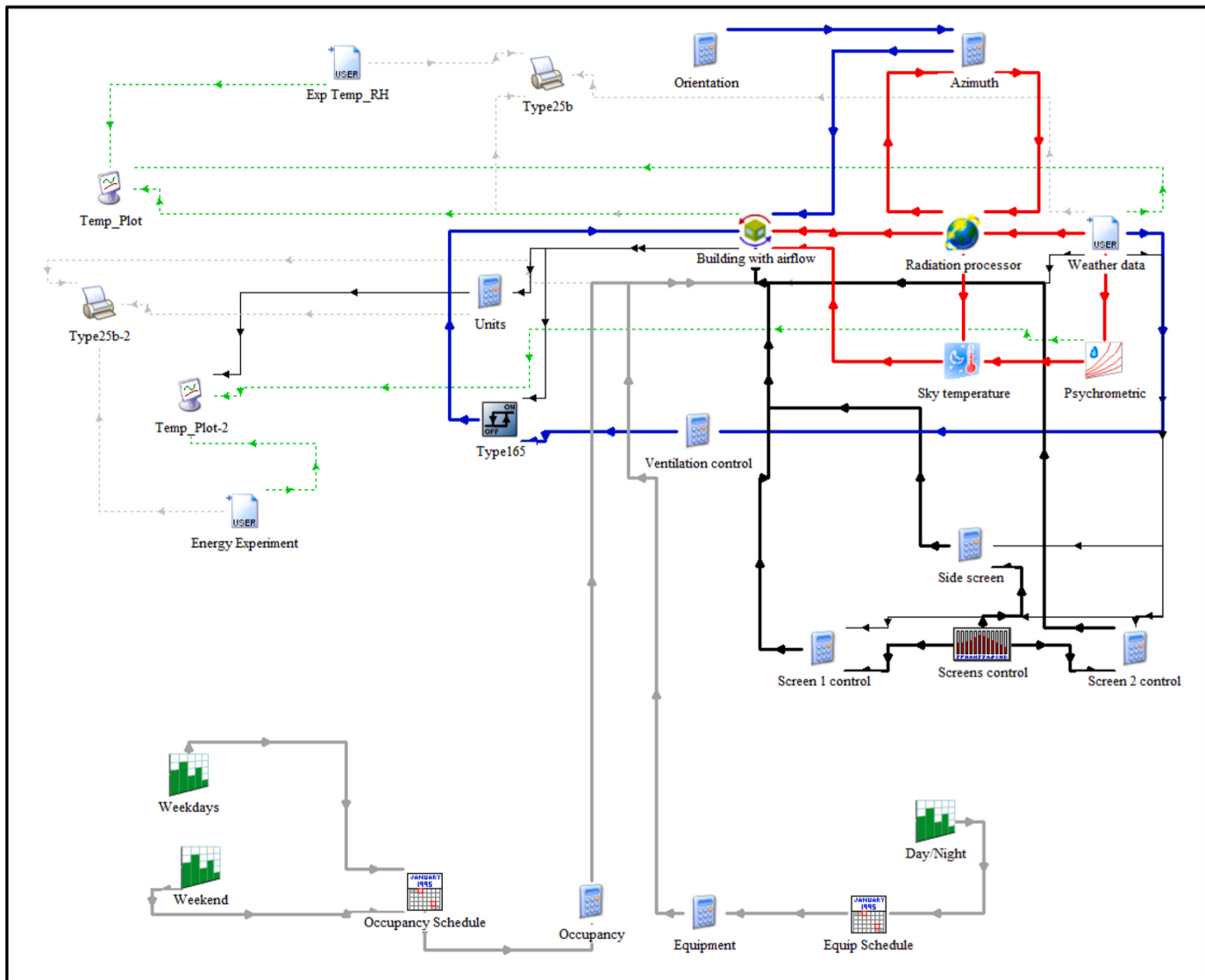


Fig. 6. TRNSYS simulation studio interface.

withdrawn, and the greenhouse has only the greenhouse-covering material that segregates the ambient and inside environment. Thus, the thermal curtains may also be closed and the two-zone scenario occurs when a thermal screen is applied. This situation represents the methods used for the single energy screen in this study, and all single-layer screens were simulated in this condition. The three-zone scenario occurs when two energy screens are applied concurrently in the greenhouse. This divides the greenhouse into zones and creates a strong buffer zone with an air gap between the two energy screens. These conditions minimize high energy exchange owing to nighttime sky radiation in each scenario, significantly affecting the quantity of nighttime energy loss and the high percentage of energy saved from the greenhouse.

Therefore, the model uses the Boolean controller simulation to regulate the inside solar radiation and temperature between  $150 \text{ Wm}^{-2}$  and  $200 \text{ Wm}^{-2}$  and  $15^\circ\text{C}$  and  $18^\circ\text{C}$ , respectively [12,49]. This research predicts the energy-saving and thermal capacity of the screen materials and quantifies the amount of energy saved when individual screens are deployed for greenhouse thermal retention to minimize excess solar radiation. To select individual screen materials in the model, the screen properties were interchanged in the model through the TRNBuild software and then updated on the TRNSYS software before running another simulation cycle.

#### 2.4. Energy saved and energy cost

Energy screens are opaque or transparent construction materials of the greenhouse that serve as main barriers within the indoor microclimate (more than a single zone; therefore, they are responsible for thermal gain or loss, which directly influences energy consumption and crop thermal comforts). The deployment of thermal screens minimizes the energy demand output and saves a significant percentage of the operation cost. The annual energy saved was determined by simulating the greenhouse model for a year to evaluate the energy demand and performance of different screens. This study calculated the energy demand for each screen, and the simulations were performed with and without the deployment of thermal screens separately. The energy demand of the greenhouse without (single zone) the application of the energy screen served as the benchmark and reference energy demand for the energy demand when an individual screen material was applied in the simulation. The calculated energy serves as the primary energy demand and is used to quantify the percentage of the energy saved for other screens. The percentage of the energy saved is calculated, and the energy cost is determined based on the energy saved predicted by the mode. The cost of the energy saved for each screen material was calculated using energy consumption by type, current energy tariffs

(energy cost), and fuel cost [17].

The energy demand predicted by the TRNSYS model provides the energy consumption values. This energy consumption is converted into energy costs using the current energy prices in South Korean markets. The simple economic viability of the screens was calculated using the energy cost based on energy carriers (i.e., electricity, diesel, gasoline, and LPG), and assumptions from previous research were adopted as shown in Table 1. To determine the energy cost, the heating efficiency, lower heating value, and gas conversion factor of 11:1 ( $\text{m}^3$  to kWh) were obtained from the literature, and electricity was converted into primary energy using a conversion factor of 2.5 [52–54]. The energy cost for electricity is calculated by the energy price 119.81 Won.  $\text{kWh}^{-1}$  and LHV of 3.599 E6 ( $\text{J.kWh}^{-1}$ ) [10,54].

The energy cost is obtained by Eqs. (12) and (13), which define the relationship between the annual fuel demand, fuel unit cost, and equivalent energy value [38].

$$C_{\text{fuel}} = \text{EEV} \times \text{AED} \quad (12)$$

$$\text{Energy Cost} = C_{\text{fuel}} \times C_e \quad (13)$$

The discounted payback period present the timeframe required to recover and recoup the initial investment cost of the screens. Energy-saving varies with indoor climate and setpoints which influences the profit. By considering the recent electricity tariff trend in South Korea, the annual tariff growth ( $r$ ) of 5% and agricultural facility interest rate ( $i$ ) of 2% were used [55,56]. The payback period of the energy saving measures was calculated by Eq. (14), [57,58].

$$DPP = \frac{\ln \left[ 1 + \frac{IC}{CF_1} \times \frac{(r-i)}{(1+i)} \right]}{\ln \left[ 1 + \frac{(r-i)}{(1+i)} \right]} \quad (14)$$

Additionally, in calculating the payback period, the prices of greenhouse screen materials were obtained from the Korean Price Information (KPI) and various manufacturing companies.

### 3. Results and discussion

#### 3.1. Properties of energy screens

##### 3.1.1. Thermophysical and aerodynamic properties

The experimental findings related to the thermophysical and aerodynamic properties of the screens are comprehensively presented in Table 2 (see Table 1). The parameters listed in the table encompass screen thickness (m), thermal conductivity ( $\text{W.m}^{-1}\text{K}^{-1}$ ), infiltration rate ( $\text{m.s}^{-1}\text{m}^{-2}$ ), screen permeability ( $\text{m}^2$ ), and simulation U-value ( $\text{W.m}^{-2}\text{K}^{-1}$ ). The results output is an evidence that the composition of screen materials plays a pivotal role in influencing its thermal conductivity. Specifically, Tempa8672, PH-77, and M2 display the highest thermal conductivities, 0.5153  $\text{W m}^{-1}\text{K}^{-1}$ , 0.5373  $\text{W m}^{-1}\text{K}^{-1}$ , and 0.6623  $\text{W m}^{-1}\text{K}^{-1}$ , respectively. This pronounced impact is influenced by the presence of aluminized strips, which exert a significant influence over the physical properties of the screen materials. These strips consist of an interwoven polyester with specific proportions. In contrast, M1 exhibits

the lowest thermal conductivity of 0.0440  $\text{W m}^{-1}\text{K}^{-1}$ . Comparatively, the thermal conductivity of Luxous1547 was 0.0458  $\text{W m}^{-1}\text{K}^{-1}$ , which is similar to 0.050  $\text{W m}^{-1}\text{K}^{-1}$  and 0.0463  $\text{W m}^{-1}\text{K}^{-1}$  reported by Refs. [3,26], respectively. Thus, the thermal conductivity of Tempa reported by Ref. [12] was 0.5200  $\text{W m}^{-1}\text{K}^{-1}$  similar to 0.5153  $\text{W m}^{-1}\text{K}^{-1}$  obtained from this research. The infiltration rate and permeability parameter serve as indicators of the material's porosity level and its capacity to restrict infiltration-related losses. Particularly, Luxous's permeability  $1.93 \cdot 10^{-11} \text{ m}$ , as reported by Ref. [36], is slightly higher than the permeability of Luxous1347 ( $1.71 \cdot 10^{-11} \text{ m}^2$ ) reported by this study. Screens M3 and Obscura notably demonstrate impermeability, signifying their possession of air-tight pore spaces that prevent air exchange. Similarly, M1 and M2 exhibit low permeability, curbing air movement through their material pores. Moreover, material thickness has a discernible impact on infiltration rates, as it impedes the free flow of air within the material's pore structure (see Table 3).

##### 3.1.2. Radiometric properties

The radiometric properties of greenhouse energy screens are influenced based on the following screen features, which include surface symmetry and asymmetric, screen layer structures, material thickness, presence of aluminized strips or aluminized surface, and homogeneity. Radiometric properties were characterized by longwave radiation and solar radiation, which involve reflectivity, transmissivity, and emissivity. The multi-layer screens M1, M2, and M3 are opaque with aluminized front surfaces with high longwave reflectance above 96% and less than 0% transmittance. However, the back surface is opaque with a white-polyester surface, this surface exhibited high emittance above 50% and reflectance below 50%, and these differences were more pronounced because of the heterogeneous nature of the multi-layer material. The asymmetric surface characteristics of the screens significantly influence screen materials with aluminized strips. This feature further categorizes the front and back surfaces into shiny (bright) and dark (dull) surfaces, respectively, owing to the different levels of their chemical compositions as they are homogenous materials. Therefore, PH-55, PH-6, PH-77, and Tempa8672 have longwave reflectance of 36 %, 58 %, 49 %, and 76 % on the front surface and 33 %, 38 %, 41 %, and 63 % on the back surface, respectively. Thus, the longwave emissivity of these same screens is 25 %, 32 %, 38 %, and 20 % on the front surface and 31 %, 52 %, 46 %, and 33 % on the back surface, respectively as presented in Table 3. These results revealed that the shining surface of energy screens enhances the longwave reflectivity, whereas a dark surface improves the longwave emissivity of any screen material. Luxous1547, PH-super, Clima45, New-Lux, and Luxous1547 are symmetric screens that exhibit similar properties (reflectance, emittance, and transmittance) under both longwave and shortwave radiation. These screens possess high transmittance and low reflectance properties when compared with other screens, and they are energy-maximization screens with high diffusion and transmissivity capacity. The longwave reflectance, transmittance, and emittance of Luxous1347 from this research are 18 %, 38 %, and 44 %, which are fairly consistent with the properties of Luxous1347 15.8 %, 38.2 %, and 46 %, respectively, as reported by Ref. [30]. These results revealed that the physical properties and chemical composition have substantial effects on the radiometric properties of energy screens.

#### 3.2. Greenhouse simulation and energy demand

Fig. 7 illustrates the daily hourly solar radiation and the ambient outside air temperature on a horizontal surface. Additionally, Fig. 8 displays the monthly dataset from the Korean Meteorological Association, showcasing the monthly minimum, average, and maximum temperatures. In specific, the minimum, maximum, and average temperature for January, June, and December, statistics are as follows:  $-15.32^\circ\text{C}$ ,  $9.36^\circ\text{C}$ , and  $-3.59^\circ\text{C}$ ;  $20.40^\circ\text{C}$ ,  $36.30^\circ\text{C}$ , and  $27.74^\circ\text{C}$ ;  $-17.8^\circ\text{C}$ ,  $13.02^\circ\text{C}$ , and  $-0.68^\circ\text{C}$ , respectively. Evidently, the lowest

**Table 1**

Unit fuel cost, lower heating value (LHV), and efficiency of each fuel type used to consider the South Korean market [38,54,59].

Fuel Type	LHV ( $\text{J.kg}^{-1}$ )	Fuel-Energy Conversion (1 L = kWh)	$\eta$ (%)	Energy Price (Korean Won. $\text{L}^{-1}$ )
Diesel	45.6 E6	1 L = 10.0	80	1534.29
Gasoline	–	1 L = 9.1	90	1631.12
LPG	46.453 E6	1 L = 6.9	88	988.44
Natural Gas	38.536 E6	1 L = 0.0088	90	0.17997

**Table 2**

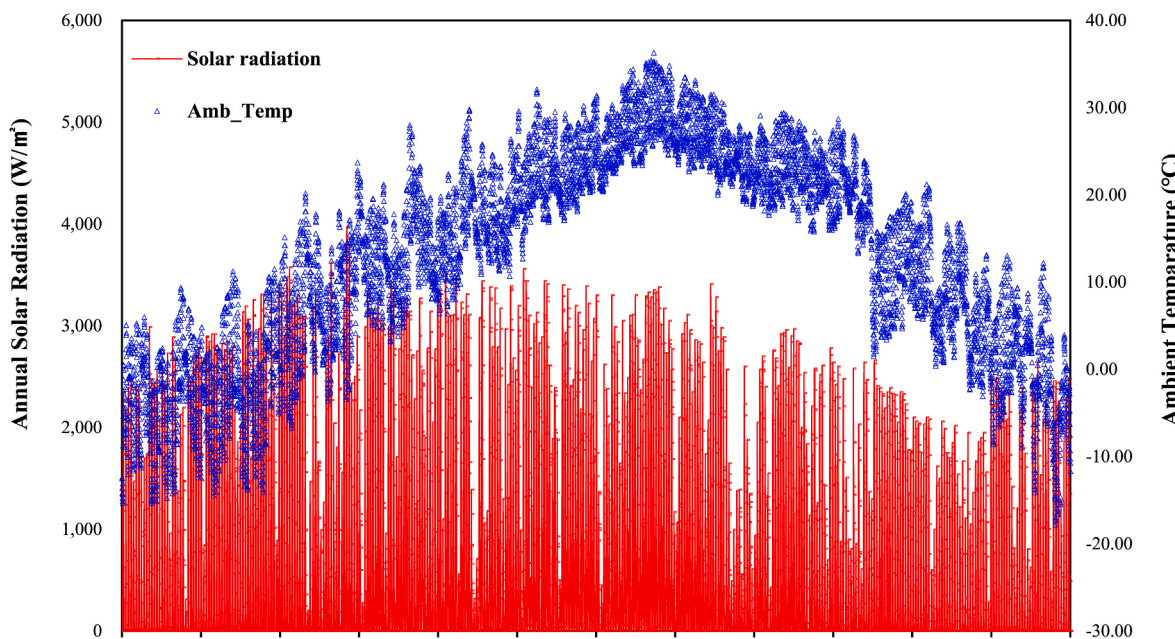
Thermophysical and aerodynamic properties of energy screens.

SN	Screen Samples	Thickness (mm)	Thermal conductivity ( $\text{W} \cdot \text{m}^{-1} \text{K}^{-1}$ )	Infiltration rate (ACH) ( $\text{m} \cdot \text{s}^{-1} \text{m}^{-2}$ )	Permeability ( $\text{m}^2$ )	U-value ( $\text{W} \cdot \text{m}^{-2} \text{K}^{-1}$ ) sim
1	White PE 300/600	0.34	0.1066	3.08	$6.51 \cdot 10^{-12}$	8.2
2	White PE 300/300	0.27	0.1078	6.97	$1.30 \cdot 10^{-11}$	8.7
3	M1	1.74	0.0440	0.06	$2.66 \cdot 10^{-13}$	3.9
4	M2	0.9	0.6623	1.00	$1.42 \cdot 10^{-12}$	5.8
5	M3	1.85	0.0486	0.00	0.00	4.6
6	Luxous1547	0.30	0.0458	4.06	$1.24 \cdot 10^{-11}$	10
7	PH-super	0.33	0.0946	7.95	$3.41 \cdot 10^{-11}$	11.5
8	New-Lux	0.25	0.0525	7.00	$1.33 \cdot 10^{-11}$	9.6
9	Clima45	0.24	0.0660	5.44	$1.49 \cdot 10^{-11}$	8.9
10	Luxous1347	0.31	0.0558	6.45	$1.71 \cdot 10^{-11}$	9.0
11	PH-55 (O)	0.41	0.1486	84.38	$7.25 \cdot 10^{-10}$	35.9
12	PH-66 (al)	0.46	0.1573	6.57	$3.41 \cdot 10^{-11}$	9.8
13	Obscura	0.34	0.3541	0.00	0.00	8.3
14	PH-77	0.37	0.5373	9.00	$2.98 \cdot 10^{-11}$	8.9
15	Tempa8672	0.31	0.5153	3.63	$1.82 \cdot 10^{-11}$	9.2

**Table 3**

Radiometric properties of energy screens.

SN	Screen Samples	Longwave Radiation						Solar Radiation			
		Reflectance		Transmittance		Emissance		Reflectance		Transmittance	
		Front	back	Front	back	Front	back	Front	back	Front	back
1	White PE 300/600	0.04	0.04	0.02	0.02	0.94	0.94	0.53	0.53	0.21	0.21
2	White PE 300/300	0.014	0.014	0.14	0.14	0.85	0.85	0.53	0.53	0.21	0.21
3	M1	0.99	0.49	0.00	0.00	0.001	0.51	0.99	0.49	0.001	0.001
4	M2	0.98	0.49	0.00	0.00	0.02	0.51	0.98	0.49	0.001	0.001
5	M3	0.99	0.49	0.00	0.00	0.01	0.51	0.99	0.49	0.001	0.001
6	Luxous1547	0.23	0.23	0.33	0.33	0.45	0.45	0.31	0.31	0.58	0.58
7	PH_super	0.02	0.02	0.38	0.38	0.60	0.60	0.29	0.29	0.66	0.66
8	New-Lux	0.30	0.27	0.26	0.308	0.45	0.42	0.30	0.25	0.58	0.57
9	Clima45	0.17	0.144	0.35	0.306	0.48	0.55	0.50	0.48	0.38	0.38
10	Luxous1347	0.18	0.18	0.38	0.38	0.44	0.44	0.3	0.25	0.58	0.57
11	PH-55 (O)	0.36	0.33	0.40	0.33	0.25	0.31	0.43	0.31	0.38	0.41
12	PH-66 (al)	0.58	0.375	0.10	0.10	0.32	0.515	0.67	0.57	0.17	0.17
13	Obscura	0.96	0.95	0.001	0.001	0.042	0.045	0.64	0.64	0.01	0.01
14	PH-77	0.49	0.41	0.14	0.14	0.38	0.46	0.62	0.55	0.13	0.12
15	Tempa8672	0.76	0.625	0.05	0.05	0.20	0.33	0.65	0.51	0.10	0.12

**Fig. 7.** Variations in daily average ambient solar radiation and air temperature for 2022.

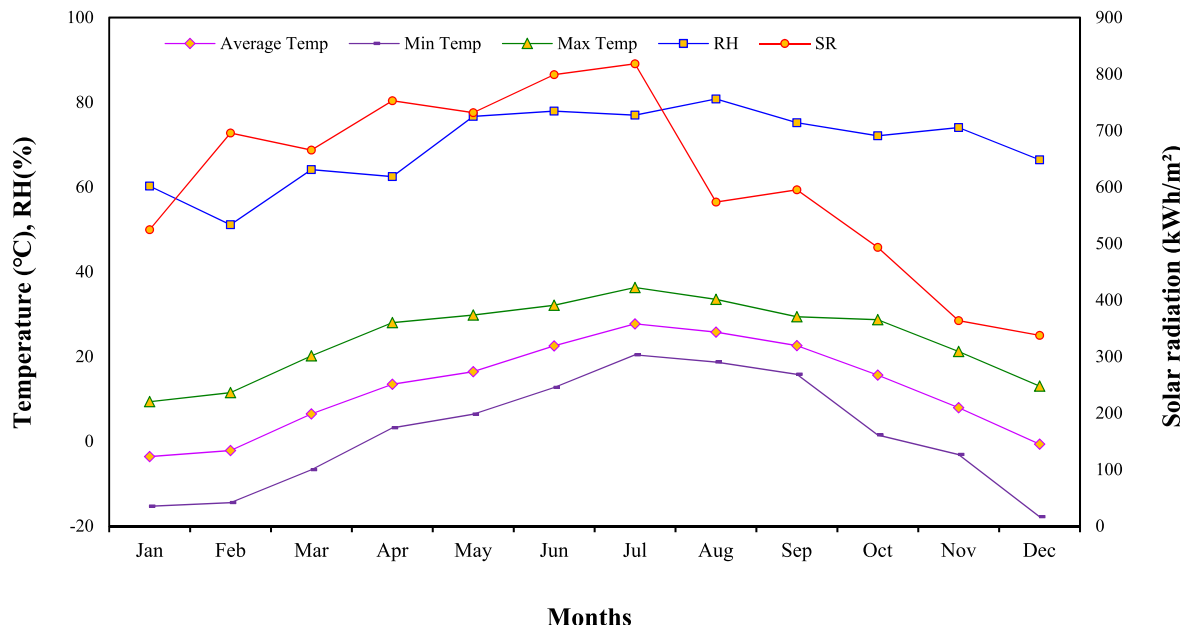


**Fig. 8.** Monthly average, daily average high and low values of ambient temperatures, and monthly average daily solar radiation in Yeouji.

temperature of the year occurred in December, measuring  $-17.8^{\circ}\text{C}$ . These graphical depictions effectively highlight the monthly fluctuations in weather conditions and their consequential impacts on greenhouse energy demands.

Fig. 9 delves into the monthly energy demand scenarios, encompassing simulations and experimental data for the greenhouse. Notably, the heating demand registered in January exceeded that of December, despite the close proximity of their lowest temperatures,  $-15.32^{\circ}\text{C}$  and  $-17.8^{\circ}\text{C}$ , respectively. This discrepancy can be attributed to the higher mean temperature experienced in January as compared to December. This observation firmly establishes the influence of the monthly average temperature as a predominant factor dictating the monthly energy requirements. Moreover, the findings unveiled a distinct scenario in June characterized by equilibrium (floating situation), wherein neither cooling nor heating was deemed necessary to maintain a stable microclimate conducive to plant growth within the greenhouse. This phenomenon owes its occurrence to the proficient shading capabilities of the climate screen, ensuring optimal conditions for greenhouse cultivation.

### 3.3. Screen energy efficiency and performance

The investigation into the energy efficiency and performance of the greenhouse energy screens was established in the exploration of their thermophysical, radiometric, and aerodynamic properties. This exploration involved the systematic interchange and selection of screens within the model to ascertain the energy retention capacity of each individual screen.

As represented in Fig. 10, the heating energy demand of the greenhouse model for the month of January was analyzed. The energy demand resulting from the greenhouse simulation was compared with the experimental demand, yielding figures of  $62,997.24 \text{ Mcal month}^{-1}$  and  $62,087.07 \text{ Mcal month}^{-1}$ , respectively. Furthermore, the simulation encompassed scenarios where the greenhouse model operated both with and without thermal screens, facilitating the quantification of actual energy consumption and the corresponding energy-saving ratios for each specific screen variant and type.

The results of the simulation highlighted distinct energy-saving ratios for different screens. Particularly, PE 300/600, White PE 300/300,

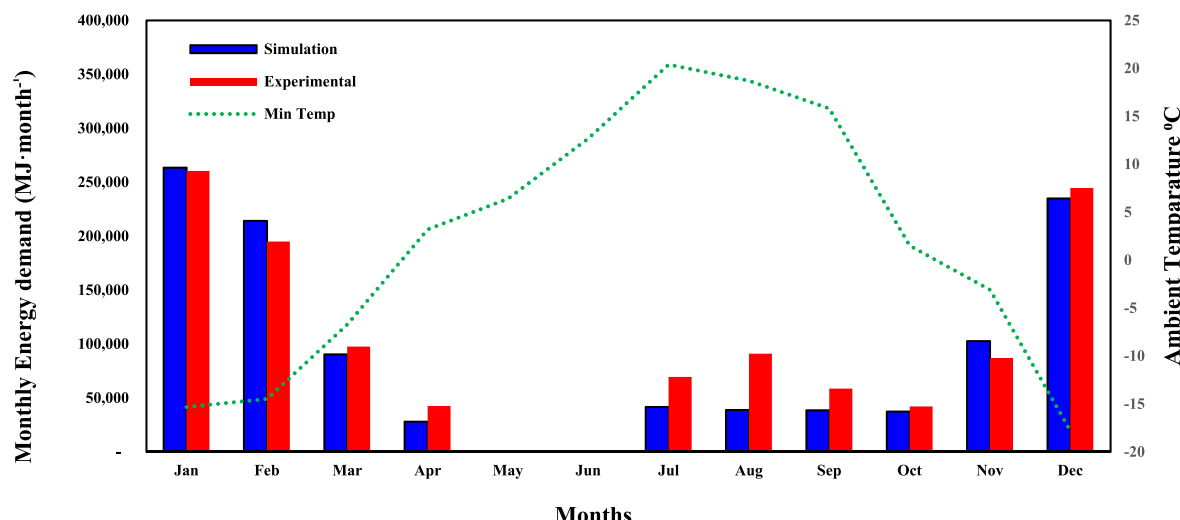


**Fig. 9.** Monthly predicted and experimental energy demand of the greenhouse throughout 2022.

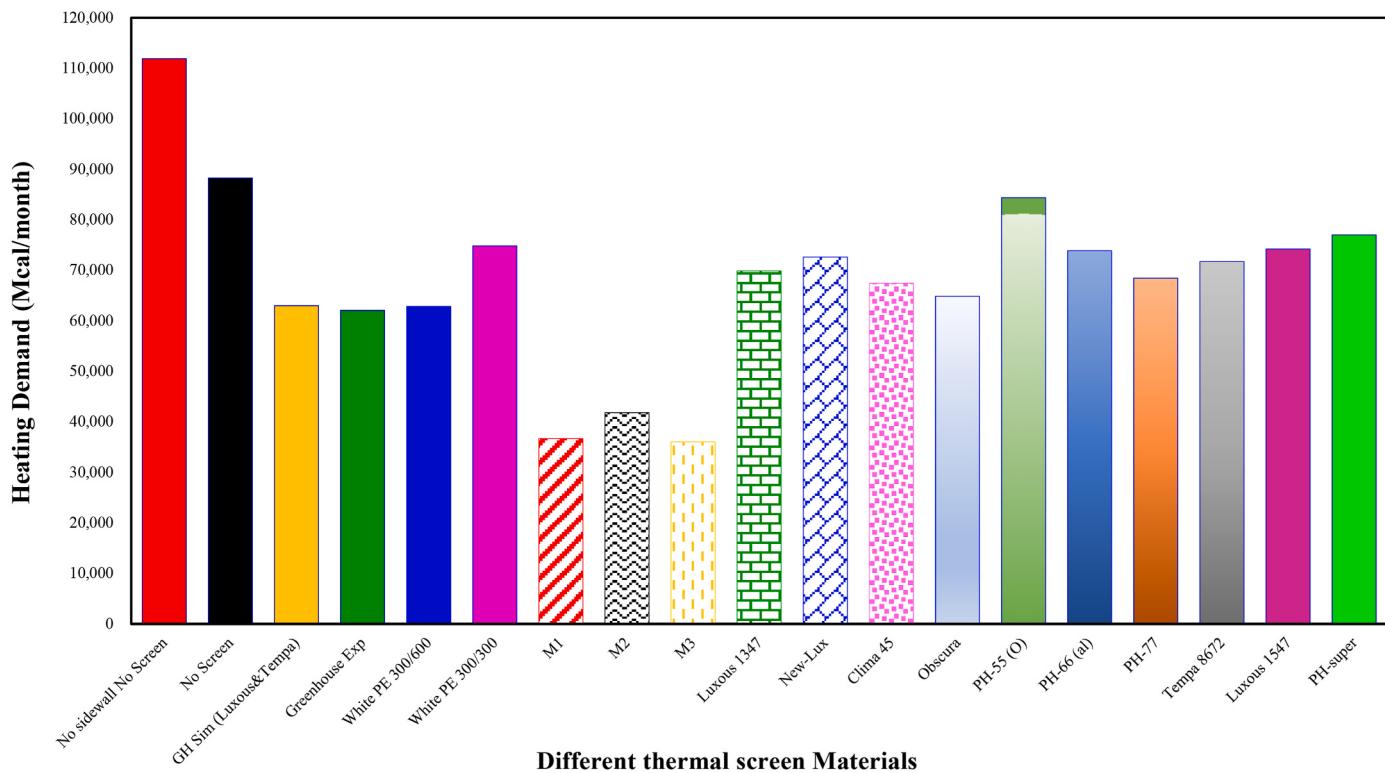


Fig. 10. Simulation results of screen materials.

M1, M2, M3, Luxous1347, New-Lux, Clima45, Obscura, PH-55(O), PH-66 (al), PH-77, Tempa8672, Luxous1547, and PH-super achieved energy savings of 28.8 %, 15.3 %, 58.4 %, 52.6 %, 59.2 %, 20.8 %, 17.7 %, 23.6 %, 26.5 %, 4.4 %, 16.3 %, 22.5 %, 18.8 %, 15.9 %, and 12.8 %, respectively, in comparison to the scenario where no climate screens were utilised. Furthermore, the results was compared with previous study [36], which reported a 32 % energy-saving percentage for the Luxous1347 screen, derived using the KASPRO software. When juxtaposed with the Luxous1347 findings from this present research, a slight variation was observed, which can be attributed to differences in permeability values exhibited by the material, which underlie the subtle disparities between the two outcomes.

In the model simulation, the PH-55 screen yielded the lowest energy-saving outcome, which can be attributed to its high porosity and open composition or nature of this material. This material's design, characterized by 45 % open strips, facilitates unhindered air movement, making it particularly effective at reducing cooling loads. Conversely, its energy-saving capacity was relatively diminished due to the nature of its porosity. On the contrary, screens M1, M2, and M3 emerged as the most energy-efficient options, possessing significant energy-saving percentages of 58.4 %, 52.6 %, and 59.2 %, respectively. This trend aligns with prior research that demonstrated similar outcomes for double-layer screens, specifically those involving an ethylene thermal screen and a chrome-coated screen. This combination led to heat loss reductions of 35 % and 47 % respectively, and a remarkable 52 % reduction when applied concurrently as a double screen [7,60]. Although, it is difficult to compare the results of these study with reported results in literature due to the diverse methods and materials used.

The higher energy retention capabilities of these screens are largely attributed to their distinct material properties, which set them apart from other options. These include impermeability, low infrared transmissivity (IR transmissivity), considerable thickness, and high emissivity. These characteristics significantly contribute to the superior energy performance exhibited by these screens. Furthermore, the study's findings emphasize that thermal blankets effectively mitigate radiative and

conductive heat losses. Additionally, screens with coated surfaces demonstrate mark significantly in reducing nighttime thermal transmittance, further enhancing their overall energy-saving capabilities.

Multi-layer screens exhibit a distinct advantage in their energy-saving capabilities due to their almost negligible infiltration rates, leading to minimal ACH. This is attributed to their tightly woven pore structure that restricts the movement of airflow, resulting in higher energy conservation when compared to other screen types. Nonetheless, examining aluminized strip screens like PH-66, PH-77, and Tempa8672, the study observed energy savings of 16.3 %, 22.5 %, and 19 %, respectively. These results align closely with the 17 % energy savings reported in a study involving Aluminet screens by Ref. [61]. Similarly, Luxous1347, New-Lux, Clima45, and Luxous1547 screens achieved energy savings of 20.8 %, 17.7 %, 23.6 %, and 15.9 % respectively. These screens exhibit properties comparable to the Sveenee thermal screen, which, in prior research, led to an 18.8 % reduction in energy consumption [7,61,62].

Considering factors such as thickness, thermal conductivity, emissivity, transmissivity, and screen permeability, it was evident that multi-layer screens showcased the lowest predicted heating energy demand. This outcome emphasizes their capacity for higher energy-savings, attributed to effective preservation of radiative, convective, and infiltration heat losses within the enclosed greenhouse space. Consequently, the utilization of multi-layer screens, primarily due to their low or nonexistent permeability, resulted in substantial reductions in infiltration heat loss. This underlines the fact that higher permeability levels correlate with increased heating demand.

### 3.4. Annual energy saved and energy cost

Fig. 11 presents a comprehensive visualization of the annual energy saved, effectively showcasing the performance of individual screens. Further insights are offered through Table 4, which presents annual energy savings and corresponding annual energy costs (based on fuel prices) per square meter, taking into account electricity, LPG, diesel, and

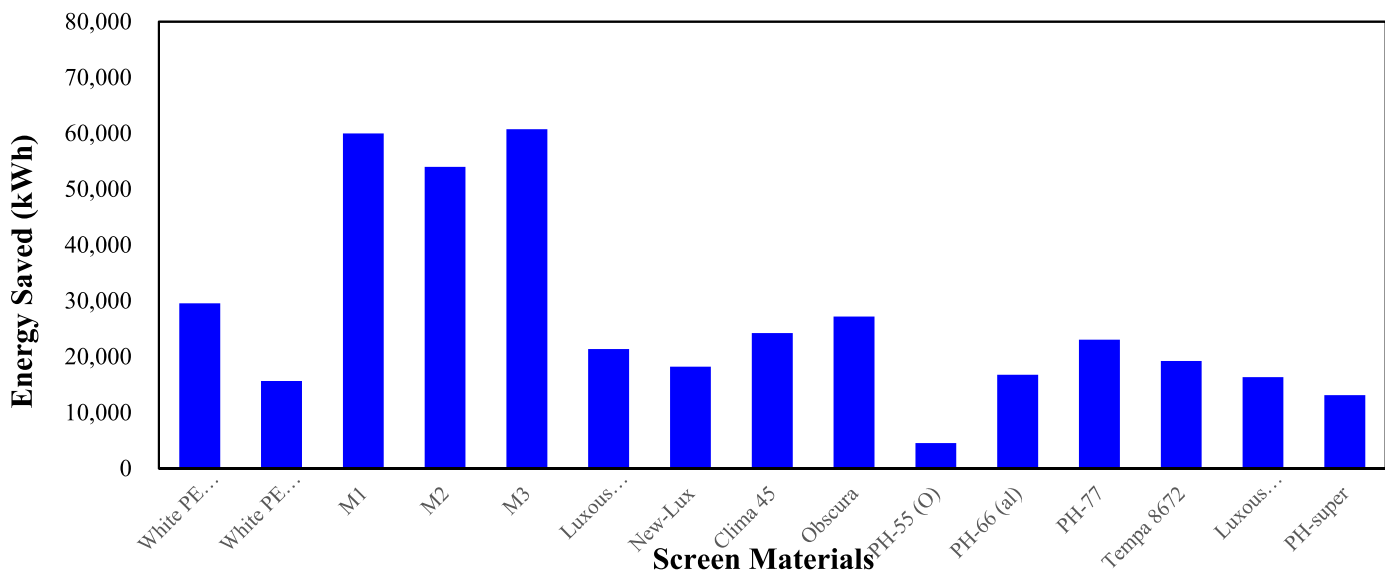


**Fig. 11.** Annual energy saved when the energy screens were applied as a single layer.

**Table 4**  
Cost of annual energy saved using greenhouse thermal screens.

SN	Screen	Energy saving (kWh)	Electricity (won.m <sup>-2</sup> )	LPG (won.m <sup>-2</sup> )	Diesel (won.m <sup>-2</sup> )	Gasoline (won.m <sup>-2</sup> )	Payback Period (year)
1	White PE 300/600	29,575.12	2186.10	2615.25	2314.91	2974.84	0.51
2	White PE 300/300	15,649.52	1156.76	1383.84	1224.92	1574.12	0.9
3	M1	59,967.56	4432.62	5302.77	4693.79	6031.89	0.86
4	M2	53,996.39	3991.25	4774.75	4226.41	5431.27	0.73
5	M3	60,747.31	4490.26	5371.72	4754.82	6110.32	0.85
6	Luxous1347	21,391.09	1581.16	1891.56	1674.33	2151.64	2.62
7	New-Lux	18,212.80	1346.23	1610.51	1425.55	1831.95	3.07
8	Clima45	24,232.21	1791.17	2142.79	1896.71	2437.42	3.08
9	Obscura	27,203.77	2010.82	2405.56	2129.30	2736.31	4.51
10	PH-55 (O)	4538.74	335.49	401.35	355.26	456.53	17.85
11	PH-66 (al)	16,759.74	1238.83	1482.02	1311.82	1685.79	5.32
12	PH-77	23,064.44	1704.85	2039.52	1805.30	2319.96	4.02
13	Tempa8672	19,242.70	1422.36	1701.58	1506.17	1935.54	3.92
14	Luxous1547	16,360.90	1209.35	1446.75	1280.60	1645.68	3.41
15	PH-super	13,132.27	970.70	1161.25	1027.89	1320.92	4.52

gasoline as energy sources. Due to their optimized thickness and minimal ACH, screens M1, M2, and M3 stand out as the top performers in terms of annual energy savings. These screens display remarkable values of  $59,967.56 \text{ kWh.yr}^{-1}$ ,  $53,996.39 \text{ kWh.yr}^{-1}$ , and  $60,747.31 \text{ kWh.yr}^{-1}$ , respectively. These figures notably exceed 100 % in energy savings compared to other materials. The efficiency of these screens is attributed to their unique properties, including thickness and minimal ACH values.

However, PH-55 (O) emerges with the least annual energy-savings, amounting to  $4538.74 \text{ kWh.yr}^{-1}$ . This screen led to the highest energy demand during simulations due to its openness and porous composition. These results collectively provide a comprehensive understanding of the energy-saving potential of various screens, with certain materials offering substantial benefits in terms of energy conservation.

Furthermore, among the group of aluminized strip screens (Aluminet), PH-77 exhibited higher performed when compared to PH-55, PH-66, and Tempa8672. PH-77 demonstrated the lowest energy demand and maximum energy saving, consequently resulting to a maximum energy cost of  $1704.85 \text{ Korean won. m}^{-2}$  for electricity. In the category of thermoreflective screens, Clima45 outperformed Luxous1347, New-Lux, PH-super, and Luxous1547. Clima45 exhibited the highest energy-saving and the maximum annual energy cost of  $1791.17 \text{ won. m}^{-2}$  for electricity. These findings further emphasize the distinct performance variations among different types of screens, underlining the significance of specific properties in determining energy-efficiency and

cost-effectiveness.

The economic cost-benefit analysis of the climate screens depends on both energy savings and local electricity tariffs. Among the available options, the M3 screen demonstrates the highest energy savings, yielding an annual cash flow of  $4490.26 \text{ won. m}^{-2}$ . Consequently, the payback period for this particular screen is remarkably short, at just 0.87 years.

### 3.5. Limitation and strength

The approach outlined in this study has certain limitations, primarily due to its exclusive applicability within the TRNSYS building energy simulation model. Consequently, its validation and usability within other building energy simulation software such as EnergyPlus and HOMER remain pending. Nevertheless, the study's notable strengths lie in the establishment of a systematic procedure and tools for quantifying a wide array of greenhouse screens. This methodology has effectively provided a clear framework for comparing different materials based on their inherent properties and real-world performance within greenhouse environments. Furthermore, the procedure's integration of energy screens into the greenhouse model stands out as a crucial step toward enhancing prediction accuracy and minimizing assumptions. This approach not only helps in reducing prediction errors but also aids in avoiding unwarranted assumptions, thereby bolstering the overall

reliability of the predictive outcomes.

#### 4. Conclusion

This research has effectively developed a methodological framework and tools for analysing the properties of diverse greenhouse screen materials, as well as their thermal and energy performance. This process enables the evaluation of the energy retention capacity of various greenhouse climate screens within the TRNSYS model, by considering the screens' thermophysical, radiometric, and aerodynamic properties. These screens properties play a crucial role in examining the annual energy demand and energy-savings.

The findings of this study unveiled that energy-efficient screens implemented in greenhouse have the potential to yield energy-saving of up to 60 % in winter for South Korean greenhouse operations. Notably, multi-layer screen materials demonstrated outstanding thermal retention capacities, with screen permeability playing a pivotal role in influencing the Air Changes per Hour (ACH), which in turn directly impacts radiative and convective heat dissipation. By considering factors such as thickness, thermal conductivity, emissivity, transmissivity, and screen permeability in relation to energy-saving potential of these materials, it was observed that multi-layer screen configurations exhibited the lowest heating demand prediction. This suggests that higher energy-savings were achieved due to the effective conservation of radiative, convective, and infiltration heat losses within the enclosed space of the greenhouse. The significant reduction in infiltration heat loss, attributed to the low or negligible permeability of these screen materials, led to the attainment of superior energy-savings using multi-layer screens.

This research study conclusively established that the M3 screen exhibited the most impressive energy-saving potential, achieving an exceptional energy retention rate of approximately 60 %. Specifically, when this screen was integrated into the simulation, it led to a recorded heating demand of 36,023.73 Mcal month<sup>-1</sup> in January. The outcome also revealed an annual energy conservation of 60.75 MWh. yr<sup>-1</sup>, which equates to a substantial energy cost reduction of 8,001,636.14 Korean Won attributed to electricity savings. The heightened thermal efficiency of screen M3 can be attributed to several factors, including a low infiltration rate, the screen's asymmetrical design (characterized by high reflectance on the front surface and high emittance on the back surface), low thermal conductivity, and considerable thickness.

Additionally, the single-layer screens Clima45 and PH-77, both featuring thermoreflective and aluminized strips, demonstrated energy savings of 23.6 % and 22.5 % respectively. The annual energy conservation figures for these screens were measured at 13.60 kWh. m<sup>-2</sup> and 12.94 kWh. m<sup>-2</sup>, accompanied by annual energy cost reductions (for electricity) of 1791.17 Korean Won. m<sup>-2</sup> and 1704.85 Korean Won. m<sup>-2</sup>, respectively. These outcomes substantiate that utilizing single-layer screens can result in a notable 20 % to about 25 % reduction in energy consumption.

In summary, the utilization of the TRNSYS software proves invaluable for evaluating the energy-saving capabilities of energy-efficient screens in greenhouses, enabling the determination of annual energy-savings and associated energy costs. The thermal performance insights gathered from these screens shed light on their capacities and attributes that directly impact their efficiency. These findings hold the potential to serve as valuable guidelines for researchers, designers and agricultural practitioners, fostering the development of sustainable agricultural systems at large.

#### Funding

This work was supported by Korea Institute of Planning and Evaluation for Technology in Food, Agriculture, Forestry (IPEF) through Agriculture, Food and Rural Affairs Convergence Technologies Program for Educating Creative Global Leader, funded by Ministry of Agriculture,

Food and Rural Affairs (MAFRA) (717001–7). This research was supported by Basic Science Research Program through the National Research Foundation of Korea (NRF), funded by the Ministry of Education [NRF-2019R1I1A3A01051739].

#### CRediT authorship contribution statement

**Anis Rabiu:** Conceptualization, Methodology, Formal analysis, Writing – original draft, Investigation, Software, Visualization. **Misbaudeen Aderemi Adesanya:** Investigation, Software, Writing – review & editing. **Wook-Ho Na:** Investigation, Resources, Data curation, Visualization. **Qazeem O. Ogunlowo:** Investigation, Validation, Writing – review & editing. **Timothy D. Akpenpuun:** Investigation, Resources, Data curation, Writing – review & editing. **Hyeon Tae Kim:** Resources, Project administration, Funding acquisition. **Hyun-Woo Lee:** Resources, Writing – review & editing, Supervision, Project administration, Funding acquisition.

#### Declaration of competing interest

The authors declare that they have no known competing financial interests or personal relationships that could have appeared to influence the work reported in this paper.

#### Data availability

Data will be made available on request.

#### References

- [1] Choab N, Allouhi A, El Maakoul A, Kousksou T, Saadeddine S, Jamil A. Review on greenhouse microclimate and applications: design parameters, thermal modeling and simulation, climate controlling technologies. *Sol Energy* 2019;191:109–37. <https://doi.org/10.1016/j.solener.2019.08.042>.
- [2] Cuce E, Harjunowibowo D, Cuce PM. Renewable and sustainable energy saving strategies for greenhouse systems: a comprehensive review. *Renew Sustain Energy Rev* 2016;64:34–59. <https://doi.org/10.1016/j.rser.2016.05.077>.
- [3] Rasheed A, Na WH, Lee JW, Kim HT, Lee HW. Development and validation of air-to-water heat pump model for greenhouse heating. *Energies* 2021;14. <https://doi.org/10.3390/en14154714>.
- [4] Lin T, Goldsworthy M, Chavan S, Liang W, Maier C, Ghannoum O, et al. A novel cover material improves cooling energy and fertigation efficiency for glasshouse eggplant production. *Energy* 2022;251:123871. <https://doi.org/10.1016/j.energy.2022.123871>.
- [5] Rasheed A, Kwak CS, Kim HT, Lee HW. Building energy an simulation model for analyzing energy saving options of multi-span greenhouses. *Appl Sci* 2020;10: 1–23. <https://doi.org/10.3390/app10196884>.
- [6] Shen Y, Wei R, Xu L. Energy consumption prediction of a greenhouse and optimization of daily average temperature. *Energies* 2018;11. <https://doi.org/10.3390/en11010065>.
- [7] Ahamed MS, Guo H, Tanino K. Energy saving techniques for reducing the heating cost of conventional greenhouses. *Biosyst Eng* 2019;178:9–33. <https://doi.org/10.1016/j.biosystemseng.2018.10.017>.
- [8] Iddio E, Wang L, Thomas Y, McMorrow G, Denzer A. Energy efficient operation and modeling for greenhouses: a literature review. *Renew Sustain Energy Rev* 2020; 117:109480. <https://doi.org/10.1016/j.rser.2019.109480>.
- [9] Yano A, Cossi M. Energy sustainable greenhouse crop cultivation using photovoltaic technologies. *Renew Sustain Energy Rev* 2019;109:116–37. <https://doi.org/10.1016/j.rser.2019.04.026>.
- [10] Choi BE, Shin JH, Lee JH, Kim HJ, Kim SS, Cho YH. Energy performance evaluation and economic analysis of insulation materials of office building in Korea. *Adv Civ Eng* 2018;2018. <https://doi.org/10.1155/2018/9102391>.
- [11] Hung Anh LD, Pásztor Z. An overview of factors influencing thermal conductivity of building insulation materials. *J Build Eng* 2021;44:102604. <https://doi.org/10.1016/j.jobe.2021.102604>.
- [12] Adesanya MA, Na WH, Rabiu A, Ogunlowo QO, Akpenpuun TD, Rasheed A, et al. TRNSYS simulation and experimental validation of internal temperature and heating demand in a glass greenhouse. *Sustain Times* 2022;14:1–31. <https://doi.org/10.3390/su14148283>.
- [13] Ahamed MS, Guo H, Tanino K. Energy-efficient design of greenhouse for Canadian Prairies using a heating simulation model. *Int J Energy Res* 2018;42:2263–72. <https://doi.org/10.1002/er.4019>.
- [14] De Zwart HF. Analyzing energy-saving options in greenhouse cultivation using a simulation model. The Netherlands.: Ph.D. Dissertation, Agricultural University Of Wageningen; 1996.

- [15] Raimundo A, Saraiva N, Dias Pereira L, Rebelo A. Market-oriented cost-effectiveness and energy analysis of Windows in Portugal. *Energies* 2021;14:3720. <https://doi.org/10.3390/en14133720>.
- [16] Frangi P, Piatti R, Amoroso G, Frangi P, et al. Evaluation of different screens for energy saving in the greenhouse. *Acta Hortic* 2011;893:275–80. <https://doi.org/10.17660/actahortic.2011.893.22>. 2011.
- [17] Lee C, Costola D, Loonen R, Hensen J. Energy saving potential of long-term climate adaptive greenhouse shell. In: Proc. BS 2013 13th conf. Int. Build. Perform. Simul. Assoc.; 2013. p. 954–61. <https://doi.org/10.26868/25222708.2013.1526>.
- [18] Gavrila S, Gontean A. Greenhouse energy balance modeling review and perspectives. IFAC Proc 2010;10:162–6. <https://doi.org/10.3182/20101006-2-pl-4019.00031>.
- [19] Altes-Buch Q, Quoilin S, Lemort V. Greenhouses: a modelica library for the simulation of greenhouse climate and energy systems. Proc. 13th Int. Model. Conf. Regensburg, Ger. March 4–6 2019;157:533–42. <https://doi.org/10.3384/ecp19157533>. 2019.
- [20] Dieleman JA, Hemming S. Energy saving: from engineering to crop management. *Acta Hortic* 2011;893:65–73. <https://doi.org/10.17660/ActaHortic.2011.893.2>.
- [21] Kumar KS, Tiwari KN, Jha MK. Design and technology for greenhouse cooling in tropical and subtropical regions: a review. *Energy Build* 2009;41:1269–75. <https://doi.org/10.1016/j.enbuild.2009.08.003>.
- [22] Vitoshkin H, Barak M, Shenderey C, Haslavsky V, Arbel A. Improving greenhouse insulation through multilayer thermal screens using the hot box method. Proc World Congr Mech Chem Mater Eng 2019;8–11. <https://doi.org/10.11159/hff19.124>.
- [23] Vitoshkin H, Haslavsky V, Barak M, Ziffer E, Arbel A. Numerical and experimental investigation of heat transfer across semi-transparent horizontal screen layers. *J Build Eng* 2021;42:103082. <https://doi.org/10.1016/j.jobe.2021.103082>.
- [24] Taki M, Ajabshirchi Y, Ranjbar SF, Rohani A, Matloobi M. Modeling and experimental validation of heat transfer and energy consumption in an innovative greenhouse structure. *Inf Process Agric* 2016;3:157–74. <https://doi.org/10.1016/j.inpa.2016.06.002>.
- [25] Ahamed MS, Guo H, Tanino K. Modeling heating demands in a Chinese-style solar greenhouse using the transient building energy simulation model TRNSYS. *J Build Eng* 2020;29:101114. <https://doi.org/10.1016/j.jobe.2019.101114>.
- [26] Rasheed A, Na WH, Lee JW, Kim HT, Lee HW. Optimization of greenhouse thermal screens for maximized energy conservation. *Energies* 2019;12:1–20. <https://doi.org/10.3390/en12193592>.
- [27] Vera-García F, Rubio-Rubio JJ, López-Belchí A, Hontoria E. Modelling and real-data validation of a logistic centre using TRNSYS®: influences of the envelope, infiltrations and stored goods. *Energy Build* 2022;275. <https://doi.org/10.1016/j.enbuild.2022.112474>.
- [28] Choab N, Allouhi A, Maakoul A El, Kousksou T, Saadeddine S, Jamil A. Effect of greenhouse design parameters on the heating and cooling requirement of greenhouses in Moroccan climatic conditions. *IEEE Access* 2021;9:2986–3003. <https://doi.org/10.1109/ACCESS.2020.3047851>.
- [29] Rafiq A, Na WH, Rasheed A, Lee JW, Kim HT, Lee HW. Measurement of longwave radiative properties of energy-saving greenhouse screens. *J Agric Eng* 2021;52:395–403. <https://doi.org/10.4081/jae.2021.1209>.
- [30] Rafiq A, Na WH, Rasheed A, Kim HT, Lee HW. Determination of thermal radiation emissivity and absorptivity of thermal screens for greenhouse. *Prot Hortic Plant Fact* 2019;28:311–21. <https://doi.org/10.12791/KSBECC.2019.28.4.311>.
- [31] Baneshi M, Gonomi H, Maruyama S. Wide-range spectral measurement of radiative properties of commercial greenhouse covering plastics and their impacts into the energy management in a greenhouse. *Energy* 2020;210:118535. <https://doi.org/10.1016/j.energy.2020.118535>.
- [32] Feuilloley P, Issanchou G. Greenhouse covering materials measurement and modelling of thermal properties using the hot box method, and condensation effects. *J Agric Eng Res* 1996;65:129–42. <https://doi.org/10.1006/jaer.1996.0085>.
- [33] Rasheed A, Lee JW, Lee HW. Development of a model to calculate the overall heat transfer coefficient of greenhouse covers. *Spanish J Agric Res* 2018;15:e0208. <https://doi.org/10.5424/sjar.2017154-10777>.
- [34] Papadakis G, Briassoulis D, Scarascia Mugnozza G, Vox G, Feuilloley P, Stoffers JA. Radiometric and thermal properties of, and testing methods for, greenhouse covering materials. *J Agric Eng Res* 2000;77:7–38. <https://doi.org/10.1006/jaer.2000.0525>.
- [35] Rabiu A, Na W, Akpenpuun TD, Rasheed A, Adesanya MA, Ogunlowo QO, et al. Determination of overall heat transfer coefficient for greenhouse energy-saving screen using Trnsys and hotbox. *Biosyst Eng* 2022;217:83–101. <https://doi.org/10.1016/j.biosystemseng.2022.03.002>.
- [36] Hemming S, Baeza E, Mohammadkhani V, Van Breugel B. Energy saving screen materials 2017;94.
- [37] Asdrubali F, Baldinelli G. Thermal transmittance measurements with the hot box method: calibration, experimental procedures, and uncertainty analyses of three different approaches. *Energy Build* 2011;43:1618–26. <https://doi.org/10.1016/j.enbuild.2011.03.005>.
- [38] Malka L, Kuriqi A, Haxhimusa A. Optimum insulation thickness design of exterior walls and overhauling cost to enhance the energy efficiency of Albanian's buildings stock. *J Clean Prod* 2022;381:135160. <https://doi.org/10.1016/j.jclepro.2022.135160>.
- [39] Balocco C, Mercatelli L, Azzali N, Meucci M, Grazzini G. Experimental transmittance of polyethylene films in the solar and infrared wavelengths. *Sol Energy* 2018;165:199–205. <https://doi.org/10.1016/j.solener.2018.03.011>.
- [40] Al-Helal IM, Abdel-Ghany AM. Energy partition and conversion of solar and thermal radiation into sensible and latent heat in a greenhouse under arid conditions. *Energy Build* 2011;43:1740–7. <https://doi.org/10.1016/j.enbuild.2011.03.017>.
- [41] Baeza E, Hemming S, Stanghellini C. Materials with switchable radiometric properties: could they become the perfect greenhouse cover? *Biosyst Eng* 2020;193:157–73. <https://doi.org/10.1016/j.biosystemseng.2020.02.012>.
- [42] Castellano S, Starace G, De Pascalis L, Lippolis M, Scarascia-Mugnozza G. Experimental results on air permeability of agricultural nets. *J Agric Eng* 2016;47:134–41. <https://doi.org/10.4081/jae.2016.542>.
- [43] Castellano S, Starace G, De Pascalis L, Lippolis M, Scarascia Mugnozza G. Test results and empirical correlations to account for air permeability of agricultural nets. *Biosyst Eng* 2016;150:131–41. <https://doi.org/10.1016/j.biosystemseng.2016.07.007>.
- [44] Miguel AF. Airflow through porous screens: from theory to practical considerations. *Energy Build* 1998;28:63–9. [https://doi.org/10.1016/S0378-7788\(97\)00065-0](https://doi.org/10.1016/S0378-7788(97)00065-0).
- [45] Takhanov D. Forchheimer model for non-Darcy flow in porous media and fractures. Department:1–31, MSc Thesis, Department of Earth Sciences and Engineering, Center for Petroleum Studies, Imperial College; 2011.
- [46] Valera DL, Álvarez AJ, Molina FD. Aerodynamic analysis of several insect-proof screens used in greenhouses. *Spanish J Agric Res* 2006;4:273–9. <https://doi.org/10.5424/sjar/2006044-204>.
- [47] Love J, Wingfield J, Smith AZP, Biddulph P, Oreszczyn T, Lowe R, et al. 'Hitting the target and missing the point': analysis of air permeability data for new UK dwellings and what it reveals about the testing procedure. *Energy Build* 2017;155:88–97. <https://doi.org/10.1016/j.enbuild.2017.09.013>.
- [48] Rigakis N, Katsoulas N, Teitel M, Bartzanas T, Kittas C. A simple model for ventilation rate determination in screenhouses. *Energy Build* 2015;87:293–301. <https://doi.org/10.1016/j.enbuild.2014.11.057>.
- [49] Trnsys SCL. Sol Energy Lab Univ Wisconsin-Madison 2018;3:7–36.
- [50] Abdel-Ghany AM, Al-Helal IM, Shady MR, Ibrahim AA. Convective heat transfer coefficients between horizontal plastic shading nets and air. *Energy Build* 2015;93:119–25. <https://doi.org/10.1016/j.enbuild.2015.02.010>.
- [51] Ozgener O, Hepbasli A. Experimental investigation of the performance of a solar-assisted ground-source heat pump system for greenhouse heating. *Int J Energy Res* 2005;29:217–31. <https://doi.org/10.1002/er.1049>.
- [52] Iweh CD, Gyamfi S, Tanyi E, Effah-Donyina E. Economic viability and environmental sustainability of a grid-connected solar PV plant in Yaounde - Cameroon using RETScreen expert. *Cogent Eng* 2023;10. <https://doi.org/10.1080/23311916.2023.2185946>.
- [53] Kim HK, Kang GC, Moon JP, Lee TS, Oh SS. Estimation of thermal performance and heat loss in plastic greenhouses with and without thermal curtains. *Energies* 2018;11:14–8. <https://doi.org/10.3390/en11030578>.
- [54] Petrol G. South Korea fuel prices, electricity prices, natural gas prices. [https://www.globalpetrolprices.com/South-Korea/electricity\\_prices/](https://www.globalpetrolprices.com/South-Korea/electricity_prices/). [Accessed 2 November 2022].
- [55] KPI. The Korean Price information and agency. <https://www.kpi.or.kr/www/contents/>. [Accessed 8 September 2023].
- [56] Nonhyup. Agricultural comprehensive fund overview. 2023. <https://seonjin.nonghyup.com/user/indexSub.do?codyMenuSeq=27053102&siteId=seonjin>. [Accessed 8 September 2023].
- [57] Gorshkov AS, Vatin NI, Rymkevich PP, Kydrevich OO. Payback period of investments in energy saving. *Mag Civ Eng* 2018;78:65–75. <https://doi.org/10.18720/MCE.78.5>.
- [58] Tushar Q, Zhang G, Bhuiyan MA, Giustozzi F, Navaratnam S, Hou L. An optimized solution for retrofitting building façades: energy efficiency and cost-benefit analysis from a life cycle perspective. *J Clean Prod* 2022;376:134257. <https://doi.org/10.1016/j.jclepro.2022.134257>.
- [59] Energy deep resource. Observing the renewable energy transition from a European perspective; Energy content of some fuels and Energy related conversion factors 2023:23. <https://deepresource.wordpress.com/2012/04/23/energy-related-conversion-factors/>.
- [60] Jolliet O, Danloy L, Gay J-B, Munday GL, Reist A. HORTICERN: an improved static model for predicting the energy consumption of a greenhouse. *Agric For Meteorol* 1991;55:265–94. [https://doi.org/10.1016/0168-1923\(91\)90066-Y](https://doi.org/10.1016/0168-1923(91)90066-Y).
- [61] Frangi P, Piatti R, Amoroso G. Evaluation of different screens for energy saving in the greenhouse. *Acta Hortic* 2011;893:275–9. <https://doi.org/10.17660/ActaHortic.2011.893.22>.
- [62] Ahamed MS, Guo H, Taylor L, Tanino K. Heating demand and economic feasibility analysis for year-round vegetable production in Canadian Prairies greenhouses. *Inf Process Agric* 2019;6:81–90. <https://doi.org/10.1016/j.inpa.2018.08.005>.